2011

Low Complexity AOFDM System for Time-varying Wireless Channels

Edwin Niroshan Christopher

Low Complexity AOFDM System for Time-varying Wireless Channels

(Spine title: Low Complexity AOFDM System for Wireless Channels)

(Thesis format: Monograph)

by

Edwin Niroshan Christopher

Graduate Program
in
Engineering Science
Department of Electrical and Computer Engineering

A thesis submitted in partial fulfillment
of the requirements for the degree of
Master of Engineering Science

School of Graduate and Postdoctoral Studies
The University of Western Ontario
London, Ontario, Canada

Certificate of Examination

THE UNIVERSITY OF WESTERN ONTARIO
SCHOOL OF GRADUATE AND POSTDOCTORAL STUDIES
CERTIFICATE OF EXAMINATION

Chief Advisors:

Dr. Jagath Samarabandu

Dr. Xianbin Wang

Examining Board:

Dr. Luiz Capretz

Dr. Lucian Ilie

Dr. Weiming Shen

The thesis by
Edwin Niroshan Christopher
entitled:
Low Complexity AOFDM System for Time-varying Wireless Channels
is accepted in partial fulfillment of the
requirements for the degree of
Master of Engineering Science

Date: _____

Chair of Examining Board
Dr. Jayshri Sabarinathan

Abstract

Signal transmitted through a wireless channel undergoes distortion due to the presence of reflectors in the environment between a transmitter and a receiver as well as due to the Doppler shift caused by the relative movement of the receiver with respect to the transmitter. Distorted signal is recovered at the receiver side by means of predicting the channel responses and performing inverse operation that the channel introduced on the transmitted signal. Prediction of channel responses becomes more complex when the receiver moves with a varying speed since it directly affects the auto-correlation of the channel responses.

First part of this thesis provides a solution for recovering the transmitted data when the receiver is moving with varying speed. The system first tracks the receiver speed variations using the number of deep fadings (nulls) in the received signal envelope of one sub-carrier during a fixed time period. If there is a significant change in receiver speed then the Kalman filter parameters are calculated and updated. Future channel responses are predicted using the updated Kalman filter parameters and used in equalizer to recover the distorted signal. The performance and computational efficiency of the proposed system outperforms the conventional system which calculates predictor parameters at a fixed interval.

Second part of the thesis presents an adaptive modulation technique based on the signal-to-noise ratio and the receiver speed. Modulation schemes for different combinations of signal-to-noise ratio and receiver speeds are obtained by selecting the higher modulation scheme with the bit error rate less than target bit error rate. Boundaries of the selected modulation schemes are found using support vector machine classifiers. The receiver uses the designed system to select appropriate modulation scheme by mapping the current modulation scheme and the channel conditions. The proposed system outperforms conventional adaptive modulation technique that uses instantaneous signa-to-noise ratio by a margin of 5 dB.

KEY WORDS:OFDM, Time-varying channel, Channel prediction, Kalman filter, Adaptive modulation, Support vector machine

Acknowledgements

I would like to acknowledge and thank my supervisors Dr. Jagath Samarabandu and Dr. Xianbin Wang for their encouragement, their very valuable analytical, practical and academic guidance and their advice throughout all aspects of my research and in the writing and publishing of this thesis. I would like to extend my thanks to Dr. Luiz Capretz, Dr. Lucian Ilie, and Dr. Weiming Shen for being the readers of this thesis and for contributing their valuable time in serving on my thesis committee.

Further, I wish to recognize the guidance and support given by my colleagues Jahidur, Viet-Ha, Sahar, Akila, Upeka, Ranga and Pubudu, the administrative staff of the Electrical and Computer Engineering Department of the University of Western Ontario, especially Sandra Vilovski.

Finally, I would like to record my deepest gratitude to my parents and brothers for their unrelenting help and encouragement for me to continue my higher education, and my sincere thanks to my good friend Dunisha and to my well wishers, Carol Wilkins and Sam Sathanatham, for motivating and encouraging me to complete my masters.

Table of Contents

List of Tables

List of Figures

Acronyms

AWGN	*Additive White Gaussian Noise*
AR	*Auto-Regressive*
BER	*Bit Error Rate*
CDMA	*Code Division Multiple Access*
DVB-T	*Digital Video Broadcasting-Terrestrial*
FFT	*Fast Fourier Transform*
FDMA	*Frequency Division Multiple Access*
FDM	*Frequency Division Multiplexing*
GWSS-US	*Gaussian Wide Sense Stationary-Uncorrelated Scattering*
IIR	*Infinite Impulse Response*
ICI	*Inter Channel Interference*
ISI	*Inter-Symbol Interference*
IDFT	*Inverse Discrete Fourier Transform*
MSE	*Mean Square Error*
MMSE	*Minimum Mean Square Error*
OFDM	*Orthogonal Frequency Division Multiplexing*
PSK	*Phase-Shift Keying*
QAM	*Quadrature Amplitude Modulation*
SNR	*Signal-to-Noise Ratio*
TDMA	*Time Division Multiple Access*
WLAN	*Wireless Local Area Networks*

Chapter 1
Introduction

1.1 Motivation

The challenge for new generation mobile radio systems is to use the available radio spectrum efficiently for high-rate and high-mobility wireless communication applications. Efficient usage of the radio spectrum is required since the bandwidth available is limited and the number of users are increasing rapidly. For many years, researchers have been looking at ways to use the available radio spectrum in a very efficient manner. In early 90's Time Division Multiple Access (TDMA) was identified over Frequency Division Multiple Access (FDMA) as providing better spectral efficiency. Later, Code Division Multiple Access (CDMA) was introduced which further improved spectral efficiency. Recently, Orthogonal Frequency Division Multiplexing (OFDM) has gained popularity over aforementioned techniques especially for the efficient use of the radio spectrum.

The fundamental limitation of wireless communication is the time-varying nature of channel fading, which results in fluctuation of the received signal power. The two main causes of the channel fading are: 1) multi-path signals where the receiver receives multiple versions of the transmitted signal due to reflection, diffraction and scattering from objects around the transmitter and receiver and 2) relative mobility of the receiver with respect to the transmitter where either the transmitter and/or the receiver and/or the objects around the transmitter and the receiver are moving. The

above two phenomena cause time and Doppler spreading which significantly affects communication system performance.

Channel equalization is used in order to overcome the time and Doppler spreadings. Equalization is a technique that recovers the distorted data by removing the fading introduced by the channel. Information about the channel (channel responses) is required at the receiver side to perform the channel equalization. Therefore, the receiver needs to predict the future channel responses so that when the signal is received, equalization can be performed on the received signal to recover the transmitted data. Time varying nature of the channel responses makes the prediction and equalization even more complex. The prediction becomes even harder when the channel parameters also vary with time.

Traditional wireless systems were usually designed for worst case scenarios which led to inefficient use of the radio spectrum. Recently, a number of researchers have attempted to track the time-varying channel parameters which are used to adaptively predict channel responses and recover distorted data at the receiver end, hence improving the spectral efficiency. Tracking of time-varying channel parameters is not only useful to recover the distorted data at the receiver side, but also to adapt good modulation scheme at the transmitter end based on the channel conditions.

This thesis considers a wireless system design with the following features: 1) effective reception of OFDM transmission through time-varying, multi-path channels when the receiver moves with random speed with respect to the transmitter and 2) effective adaptive modulation based on channel conditions and user mobility for better performance of the system.

1.2 Literature Review

Prediction of channel response in an OFDM system has been an active research area since the development and growth in popularity of OFDM. Channel prediction algorithms are categorized into following three groups based on whether they use training symbols or not:

1. Training based channel prediction [1]

   This method uses pilot symbols interspersed with the transmitted data so that the receiver can make use of these pilot symbols to learn channel conditions and to effectively recover the data. The main disadvantage of this method is bandwidth inefficiency due to the use of pilot symbols.

2. Blind channel prediction [2]

   A blind channel prediction algorithm uses the properties of the transmitted signals to estimate the channel conditions and recover the data. Disadvantages such as poor accuracy, high complexity and slow convergence have made blind channel prediction algorithms unsuitable for modern wireless communication systems even though they have high bandwidth efficiency.

3. Semi-blind channel prediction [3]

   The main objective of semi-blind channel prediction is to achieve better performance compared to blind channel prediction with the use of a few pilot symbols; hence the method is called semi-blind channel prediction. This method provides a good tradeoff between bandwidth efficiency and prediction accuracy.

1.2.1 Kalman Filter based Prediction of Channel Response

The Kalman filter algorithm is a recursive method that uses noisy measurements to estimate the state of a dynamic system. Initially,the Kalman filter was used for the estimation of time invariant channels [4]. Then it was found that the Kalman filter can be used to estimate the time varying channel parameters by modeling time varying channel states using an Auto-Regressive (AR) model [5]. Ilits and Fuxjaeger [5,6] used the time domain statistics of the wireless channel to estimate the channel parameters but they did not provide any methods to estimate the AR model parameters. This limited the application of the Kalman filter in prediction of channel responses.

Tsatsanis et al. [7] proposed a least square technique to obtain the AR model parameters based on the channel correlation using the training data. Zhou et al. [8] came up with a proposal that the channel correlation could be estimated from the second-order statistics of the output and the training symbols were not required. Auto-correlation of channel responses obtained from the second-order statistics was applied in Yule-Walker method [9] to estimate the AR model parameters. Based on those estimations of AR model parameters, the time varying channel response was predicted using the Kalman filter.

Bulumulla et al. [10] used the Kalman filter to estimate the two dimensional OFDM channel responses in the frequency domain. This algorithm utilized the time and frequency domain channel correlation and provided optimum performance at the expense of computational complexity. The computational complexity was high due to the inverse matrix calculation. Chen and Zhang [11] introduced a per-sub-carrier Kalman estimator with a frequency domain refinement which first predicted the channel responses on each sub-carrier. Then a frequency domain refinement was carried out using a frequency domain correlation to further improve the prediction

accuracy. Since the Kalman filter was applied on each sub-carrier, the matrix division that was required in the method used by Bulumulla et al. [10] was replaced by simple scalar division.

The fundamental problem in most of these prediction methods is that they apply the Doppler shift and delay spread of the channel to the equation that was obtained using a theoretical analysis to calculate the auto-correlation of the channel responses which later used for prediction of channel responses. Jakes' model is the widely used Doppler Spectrum model for Rayleigh fading channel. The theoretical auto-correlation of the channel following Jakes' model [12] spectrum was calculated using the equation (1.1)

$$r_{k,l}[m] = J_0(2\pi f_D m T)\frac{1 - j2\pi(l-k)\sigma_t/T}{1 + 4\pi^2(l-k)^2\sigma_t{}^2/T^2} \tag{1.1}$$

where f_D is the maximum Doppler shift, σ_t is the maximum delay spread of the channel, T is the OFDM symbol duration and $J_0(\cdot)$ is the zero order Bessel function of the first kind. However, on one hand, there is no guarantee that the channel will always follow the theoretical analysis and on the other hand, the calculation of the variables in the equation 1.1 involve high computational complexity. If one was to calculate the Doppler shift and then calculate the AR model parameters, it would increase the number of computations. This would result in a delay in processing and/or more power consumption. The other problem with these methods was that they assumed that the Doppler shift is constant. Authors did not consider these prediction methods when the speed of the receiver is time varying.

Prediction of channel responses for time-varying channel parameters by tracking the changes in channel parameters has become a more popular research area now. Wei Bai et al. [13] used scattered pilot symbols to track time varying channel parameters

and to predict the channels. His method involved matrix inversion as a part of the prediction process which was costly in terms of computation. Song et al. [14] used a least square tracking method to estimate time-varying Kalman filter parameters. In Song's method [14], a Kalman filter order of one was used and it became hard to track the Kalman filter parameters if the AR order is more than one. An Infinite Impulse Response (IIR) approximation of the Doppler spectrum was found by cascading a digital bi-quad and low-pass filter in the method proposed by Lee [15]. He used a training sequence to estimate the Doppler frequency and magnitude spectrum which were used for prediction of channel responses. Lee et al. [16] suggested different pilot arrangements for different mobile speeds to increase the prediction accuracy. In his method it was assumed that the receiver was aware of its speed and reported to the transmitter to adapt the allocated pilot pattern for that speed. Recently, Heidari et al. [17] came up with a channel tracking algorithm based on the prediction error threshold. If the prediction error was greater than the threshold value, then the Doppler shift was estimated using a gradient-based approximation. The estimated Doppler shift was then used to find the Kalman filter parameter for prediction.

Adaptive modulation is a technique that uses different arrangements of bits so that one or more bits can be transmitted at a time. Adaptive modulation helps to improve spectral efficiency and performance of the system by transmitting as many bits as possible when the channel condition is good and transmitting as few bits as possible when the channel condition is poor.

Adaptive modulation has been an active research area in wireless communication for the past 10 years especially as rapidly varying wireless channel conditions prompted researchers to look for effective data transmission methods. Furthermore, the independence of each sub-carrier from one another in OFDM system gave the flexibility to assign different modulation schemes for each sub-carrier [18].

The adaptive modulation schemes proposed by Goldsmith [19] and Hanzo [20] assumed that the fading channel is slowly varying but they did not take these channel fadings into consideration to determine the modulation scheme. Recently, time-varying channel fading was also taken into consideration with Signal-to-Noise Ratio (SNR) when choosing a modulation scheme [21, 22]. The instantaneous SNR (γ) measured at the receiver side is given by (1.2).

$$\gamma = \frac{\hat{H}_n^2}{N_0} \tag{1.2}$$

where H_n is the channel gain and N_0 is the noise variance. Based on this γ a modulation scheme was selected which provided an acceptable Bit Error Rate (BER) performance with high spectral efficiency. For example, if the γ was low then a lower modulation scheme (few bits per symbol) was used and if the γ was high then a higher modulation scheme was used.

Use of γ may leads to poor performance and stability issues. The γ will work well if the channel responses vary slowly (in low Doppler shift scenarios) with respect to time. This will allow sufficient time for the receiver to send the estimated channel information to the transmitter and the transmitter to decide new modulation scheme based on the γ. The channel condition will be still valid when data is transmitted with the new modulation scheme. But when the channel fading variations are high (in high Doppler shift scenarios), then the transmitter will not have sufficient time to adapt itself to channel conditions. The modulation scheme chosen may not be valid any more considering the delays associated in relaying γ back to the transmitter. Figure 1.1 shows a typical γ of a Rayleigh fading channel when the Doppler shift is 200 Hz and average noise power is -20 dB with respect to the received signal power.

The other main consideration in adaptive modulation systems is the system sta-

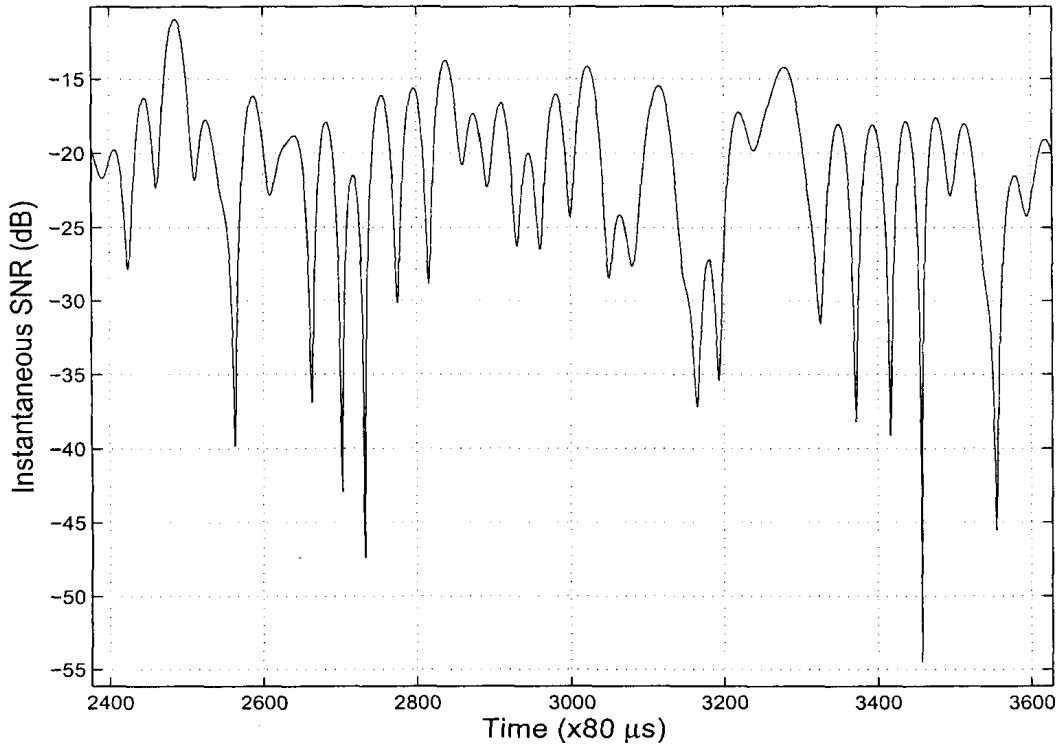

Figure 1.1: Instantaneous SNR vs time for a single carrier received signal.

bility. When there are rapid fluctuations in channel conditions or channel parameters, the modulation technique used can fluctuate between two modulation schemes in the transmitter and receiver. These fluctuations can consume more power for switching modulation schemes back and forth.

1.3 Thesis Contribution

This thesis consists of two main contributions, namely adaptive prediction of channel responses and adaptive modulation for a receiver moving with varying speed. This section elaborates the two main contributions.

First part of this thesis presents an adaptive prediction of channel responses when there is a relative motion between the transmitter and the receiver. Prediction of channel responses when the receiver moves with fixed speed with respect to the

transmitter is fairly straightforward since the Doppler shift is fixed. However, the prediction task becomes complicated when the receiver speed changes with respect to time because the Doppler shift also changes with the relative receiver speed. In order to predict the channel responses accurately, it is necessary to keep track of Doppler shift changes. A system is proposed to address this concern.

The proposed predictor system keeps track of the Doppler shift changes and updates the predictor parameters when there is a significant change. The Doppler shift changes are tracked using the envelope of the received signal based on the following property: "when considering a single carrier signal transmitted through a wireless channel whose effective bandwidth is higher than the signal bandwidth, the received signal envelope (or power) at the receiver side will have relatively deep fading around every half-wavelength ($\frac{\lambda}{2}$) distance" [23]. The proposed system makes use of number of deep fadings (here onwards called as "nulls") in the past fixed time period to keep track of the Doppler shift changes. In multi-carrier system like OFDM, the signal received at a subcarrier is considered after the removal of interference among the subcarriers.

The value of Doppler shift introduced by the channel due to the relative motion of the receiver with respect to the transmitter has different impacts on auto-correlation of the channel responses. For lower Doppler shifts, a small change in the Doppler shift will only have very little change in auto-correlation, whereas for higher Doppler shifts, a small change in Doppler shift will have drastic change in auto-correlation. The proposed system first finds any significant changes in the Doppler shift with respect to the Doppler shift at the last time instance when the auto-correlation of the channel responses were calculated. Then it calculates the auto-correlation of the channel responses and corresponding predictor parameters for future prediction. After updating the parameters, it again starts to keep track of the

next significant change in the Doppler shift based on recently updated Doppler shift.

The calculation of auto-correlation and predictor parameters only when there is a significant change provides computational efficiency for the case where the receiver is moving with a varying speed with respect to the transmitter.

The second part of this thesis discusses adaptive modulation technique based on the instantaneous SNR (γ) and the receiver speed (v_r). Since estimation of v_r involves high computation, it is replaced by the auto-correlation coefficient of channel responses at correlation index m_1 ($R_H[m_1, v_r]$) which is obtained during the process of prediction of channel responses. The value for correlation index m_1 is chosen such that $R_H[m_1, v_r]$ gives a good resolution for receiver speed and at the same time the relationship between v_r and $R_H[m_1, v_r]$ is monotonic for the speed range under consideration. Here onwards, $R_H[m_1, v_r]$ is replaced by $R_H[v_r]$ since m_1 is fixed and $R_H[v_r]$ depends only on v_r.

The proposed adaptive modulation technique makes use of the estimated γ and $R_H[v_r]$ to select a modulation scheme which provides targeted BER with maximum spectral efficiency. The proposed system makes use of a two-dimensional, non-linear classification algorithm to estimate an appropriate modulation scheme based on γ and $R_H[v_r]$. The system is trained off-line to adapt certain modulation schemes based on the γ and $R_H[v_r]$. The trained system then works by selecting a modulation scheme using estimated channel conditions.

The adaptive modulation system works on simple mapping of channel condition. Once the γ and $R_H[v_r]$ are estimated, a modulation scheme is chosen by mapping the estimated values on the two-dimensional space defined using γ and $R_H[v_r]$ to find the efficient modulation scheme. Once these parameters are estimated at the receiver side, a request is sent to the transmitter. The transmitter then assigns the requested modulation on the sub-channels used by the particular user. Furthermore,

a modification to the classification boundaries is introduced to ensure that the system stability is maintained when there are rapid fluctuations in channel conditions.

Potential applications of the proposed technique involves high-speed mobile data communication. One typical example would be video streaming in a high mobility environment such as mass transit in urban or sub-urban areas.

The overall system was divided into four separate subsystem and implemented in Matlab® R2010a. The four subsystems are OFDM transmitter, OFDM receiver with channel model, channel predictor subsystem and modulation selector subsystem. Here, the channel is modeled using the Matlab® R2010a built-in function (rayleighchan function in Communication Toolbox) with some modification to incorporate the speed changes of the receiver with respect to the transmitter and the modulation and demodulation are also done using the functions in Communication Toolbox. In the second part of the thesis, the boundary equations are obtained using the support vector machine classifier functions in Bioinformatics Toolbox. All the other systems are coded manually based on the analysis discussed on each section. The total codes size was around 5000 – 6000 lines for the overall system.

1.4 Thesis Outline

The thesis is comprised of the following five chapters. Following is a briefing of each chapter following:

Chapter 2: In the first section of chapter 2, a brief introduction of OFDM system is presented.Then an overview in modulation technique is introduced. Next, the wireless channel model that is used in this thesis is discussed. Then the prediction of channel responses and equalization techniques are introduced briefly. Finally, an overview of soft-computing techniques are introduced.

Chapter 3: In this chapter, a frequency domain prediction of channel responses and equalization using the Kalman filter for varying receiver speed is presented in detail. First, the property used to identify the receiver speed variations is analyzed. Then the detailed description of null detection algorithm along with probability of false null detection is discussed. The implementation of full adaptive prediction system is described next. Finally, the performance and the computational efficiency of the proposed system are compared with traditional systems.

Chapter 4: This chapter presents an adaptive modulation using non-linear classification and mapping based on γ_n and the receiver speed. Implementation of the proposed modulation method is discussed and followed by the system performance analysis and comparison with traditional adaptive modulation system.

Chapter 5: Conclusions and future work is presented in this chapter.

Chapter 2

Theoretical Background

2.1 Introduction

This chapter presents a basic introduction to the technologies that are used in this thesis. The topics covered are the basics of OFDM, modulation, time-varying channel models, prediction of channel responses and equalization. Some background in soft computing techniques such as the Kalman filter, first derivative test, second derivative test and non-linear classification and mapping are also introduced.

2.2 OFDM Basics

Orthogonal Frequency Division Multiplexing (OFDM) splits high rate serial data streams into multiple low-rate data streams each of which is modulated separately to sub-carriers and transmitted in parallel. In OFDM, sub-carriers are selected such that they are orthogonal to each other to reduce cross talk and inter-carrier interference (ICI). The orthogonality allows the sub-carriers to be arranged such that they are very near to each other as shown in Figure 2.1.

OFDM splits the broadband channel into multiple narrow-band channels and the symbol duration of the transmitted signals are high. This makes the bandwidth of the signal smaller when compared with the sub-channel bandwidth. Therefore, all the frequency components of the signal undergo similar fading; hence it is called

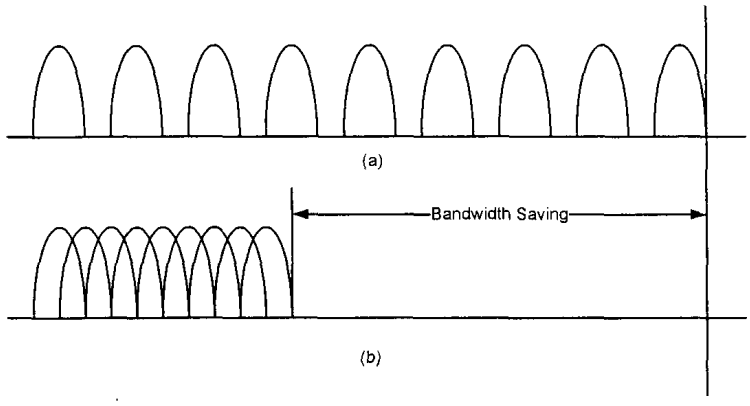

Figure 2.1: Comparison of the spectra of (a) classical parallel transmission system and (b) OFDM system [24].

'frequency-flat fading'. The data distorted by frequency flat fading can be recovered easily with simple equalization techniques.

2.2.1 Elimination of Inter-Symbol Interference (ISI)

Compared to a conventional single carrier system, OFDM suffers less Inter-Symbol Interference (ISI) caused by multi-path propagation due to its low symbol rate stream. In OFDM, ISI is eliminated by the introduction of the guard interval. The guard interval also eliminates the need for a pulse-shaping filter, and it reduces the sensitivity to time synchronization problems.

A Cyclic Prefix (CP) is transmitted during the guard interval, which is basically the last part of the same OFDM symbol [25]. The CP occupies the time interval as the guard period in frequency division multiplexing (FDM) and at the same time ensures that the delayed replica of the OFDM symbols will always have a complete symbol within the Fast Fourier Transform (FFT) window. Having the last part of the OFDM symbol as the guard interval as shown in Figure 2.2 allows the linear convolution between the signal and channel response to be replaced by a circular convolution.

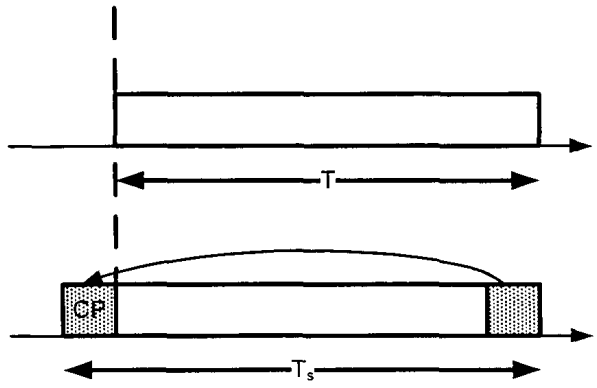

Figure 2.2: An OFDM Symbol with CP [25].

The performance of an OFDM is severely affected by the Doppler spread which causes the loss of orthogonality between sub-channels and leads to Inter Channel Interference (ICI). The main reason for the Doppler spread is receiver mobility with respect to the transmitter.

2.2.2 System Model

The standard OFDM system shown in Figure 2.3 undergo following processes at the transmitter:

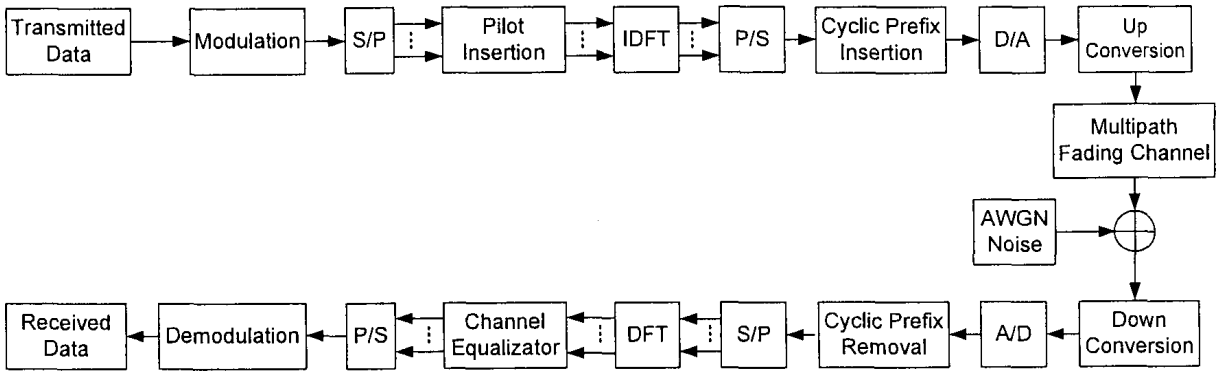

Figure 2.3: Standard OFDM System [26].

1. Serial-to-parallel alignment

Here, high data rate bit stream is divided into many (equal to number of data sub-carriers in OFDM system) low data rate bit streams.

2. Baseband modulation

   Divided data streams are modulated separately to subcarrier frequencies using M-ary Phase-Shift Keying (PSK) modulation or M-ary Quadrature Amplitude (QAM) Modulation.

3. Insertion of pilot symbols

   Predefined pilot symbols are inserted within the modulated data and are used by the receivers to keep track of the channel characteristics and recover the estimation errors of the channel responses.

4. Inverse Discrete Fourier Transform (IDFT)

   The output of the modulator in the previous step is a frequency domain discrete signal. IDFT is applied to the signal output from modulator and the result is the time domain signal:

$$x[n] = \frac{1}{N} \sum_{k=0}^{N-1} X[k] e^{(j\frac{2\pi}{N} k n)} \tag{2.1}$$

   where, N is the number of sub-carriers in the OFDM system, $X[k]$ is the base-band modulated frequency domain data and $x[n]$ time domain signal to be transmitted.

5. Cyclic Prefix (CP) Addition

   A CP is added to avoid the ISI caused by multi-path delay. The length of the CP is chosen so that it is greater than the maximum delay spread.

6. Parallel-to-serial alignment

   After the addition of the CP, the data are aligned serially to be transmitted out.

7. Up sampling to carrier frequency

   The data to be transmitted are up converted to a carrier frequency and transmitted out.

At the receiver side, data $x[n]$ transmitted through the noisy fading channel is received at the receiver side as given by the equation (2.2)

$$y[n] = h[n] * x[n] + w[n] \tag{2.2}$$

where $y[n]$ is the received signal, $h[n]$ is the fading channel response and $w[n]$ is the additive white Gaussian noise (AWGN). At the receiver side, inverse of the transmitter operations are done along with noise filtering, channel prediction and equalization.

2.3 Modulation

Modulation is a technique used to transmit one or more binary bits as one symbol. The binary bits are modulated on carrier signal and transmitted out. There are three different types of digital modulation: 1) Quadrature Amplitude Modulation (QAM), 2) Frequency Shift Keying (FSK) modulation and 3) Phase Shift Keying (PSK) modulation. A binary data modulated using a digital modulation can be shown using a constellation diagram. Constellation diagram displays the signal as a two-dimensional scatter diagram in the complex plane at symbol sampling instants.

Figure2.4 shows the constellation diagram of PSK modulated symbols. From the figure it is evident that the distance between constellation points decreases with the increase of number of bits per symbol. Therefore, the BER increases as the order of the modulation is increased and transmitted through a noisy channel.

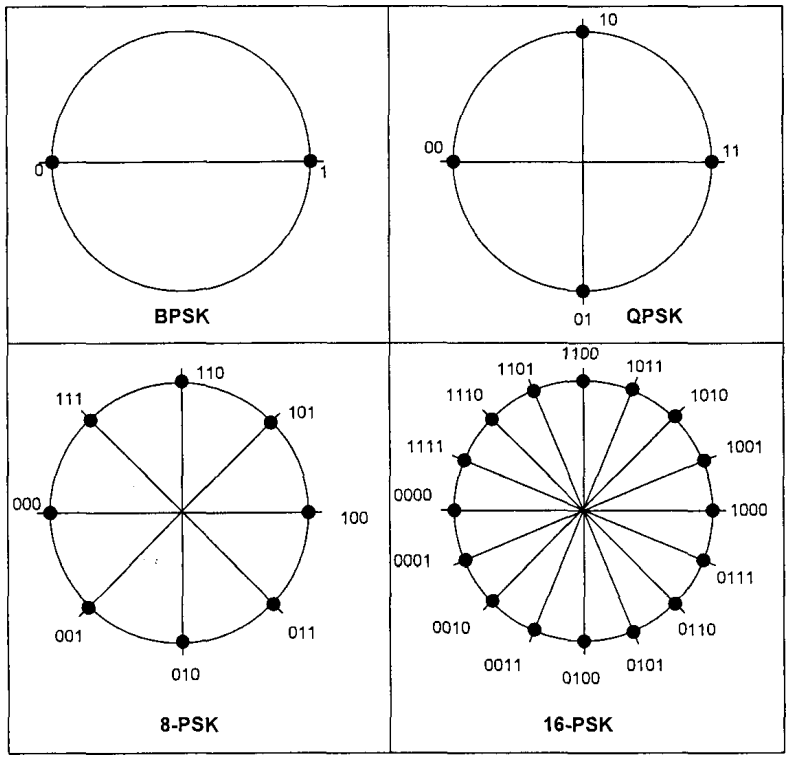

Figure 2.4: Constellation diagram of M-PSK modulation.

2.4 Wireless Channel Model

A signal transmitted through the wireless channel is subjected to distortion (or fading) due to free space loss, reflection, refraction, diffraction and scattering. The fading is categorized into three, namely: 1) large-scale fading, where fading is mainly due to the free space loss which determines the power level averaged over a large area, 2) shadowing which occurs due to objects obstructing the propagation paths between

the transmitter and the receiver and 3) small-scale fading which occurs due to small changes in spatial position of the transmitter and receiver.

The two main reasons for small-scale fading are: 1) multi-path signals received by the receiver due to reflection and scattering caused by objects around the transmitter and the receiver and 2) relative speed of the receiver with respect to the transmitter. The relative speed can be due to either 1) movement of the receiver, 2) movement of the transmitter, 3) movement of the objects around the transmitter and the receiver or 4) any combination of above three.

2.4.1 Multi-path Effects

Multi-path reception occurs mainly due to the reflection and scattering of the transmitted signal from the objects around the transmitter and the receiver. The signal received by the receiver is the accumulation of different delayed and modified versions of the transmitted signals. Therefore, the received signal may give good or poor reception based on the received multi-path signals and their direction. The received power varies related to the position of the receiver with respect to the transmitter.

Based on multi-path reception, small-scale fading can be further categorized into: 1) frequency-flat fading and 2) frequency-selective fading. Frequency-flat fading occurs when the coherence bandwidth (B_c) of the channel is larger than the signal bandwidth; therefore all the frequency components of the signal undergo similar fading. Frequency-selective fading arises when the B_c is smaller than the signal bandwidth and the different frequency components undergo different fading. Here, coherence bandwidth (B_c) is a statistical measure of the range of frequencies over which a channel passes all the spectral components with almost equal gain and linear

phase. Figure 2.5 [23] shows the effects of different types of fading on a transmitted signal in the time and the frequency domains.

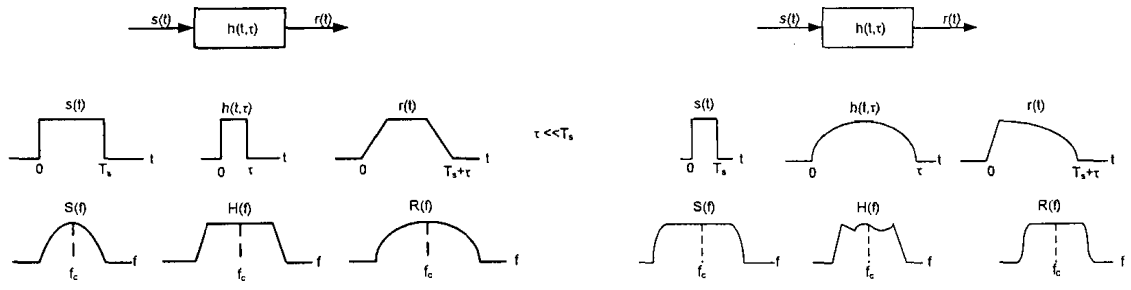

Figure 2.5: (a) Flat fading and (b) frequency-selective fading characteristics [23].

2.4.2 Doppler Effects

The received signal frequency differs from that of the transmitted signal when there is receiver movement relative to the transmitter. This phenomenon is called the Doppler Effect. The change in frequency is called Doppler shift. It depends on relative speed of the receiver, transmission frequency and direction of movement. The Doppler shift f_d observed by the receiver is given by:

$$f_d = \frac{v}{\lambda} cos(\theta) \tag{2.3}$$

The maximum Doppler shift f_D is given by:

$$f_D = \frac{v}{\lambda} \tag{2.4}$$

where v is the relative speed of the receiver with respect to the transmitter, λ is the wavelength of the transmitted signal and θ is the angle of arrival of the received signal.

Here, λ can be written as

$$\lambda = \frac{c}{F_c} \tag{2.5}$$

where c is speed of the light and F_c is the carrier frequency of the transmitted signal.

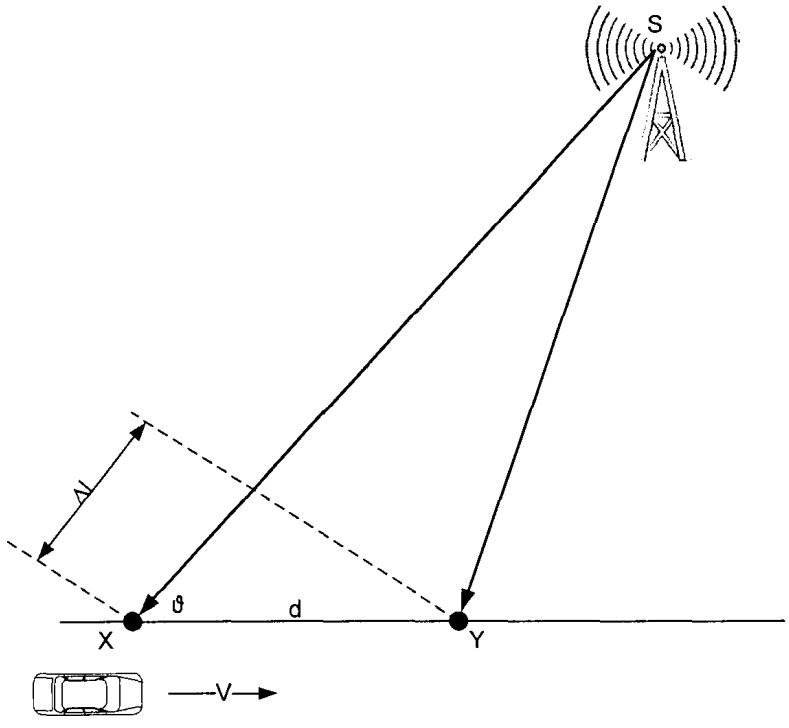

Figure 2.6: Doppler shift phenomenon.

The duality of the Doppler shift, i.e. Coherence time (T_c), is the time duration over which the channel impulse responses are essentially time invariant. The T_c and f_D are inversely proportional to each other. That is,

$$T_c \approx \frac{1}{f_D} \tag{2.6}$$

If T_c is defined as the time over which the time correlation function is above 0.5, then the coherence time is approximately [27].

$$T_c \approx \frac{9}{16\pi f_D} \tag{2.7}$$

Using the equations (2.6) and (2.7) T_c can be defined as

$$T_c = \sqrt{\frac{9}{16\pi f_D^2}} = \frac{0.423}{f_D} \tag{2.8}$$

If the symbol period of the baseband signal is greater than the coherence time then the signal will be distorted. Depending on the symbol period and coherence time, small scale fading can be categorized into: 1) fast-fading, where the rate of change of channel is larger than the rate of change of transmitted signal and 2) slow fading, where the rate of change of channel is smaller than the rate of change of transmitted signal. Figure 2.7 [23] shows the categorization of the small scale fading types.

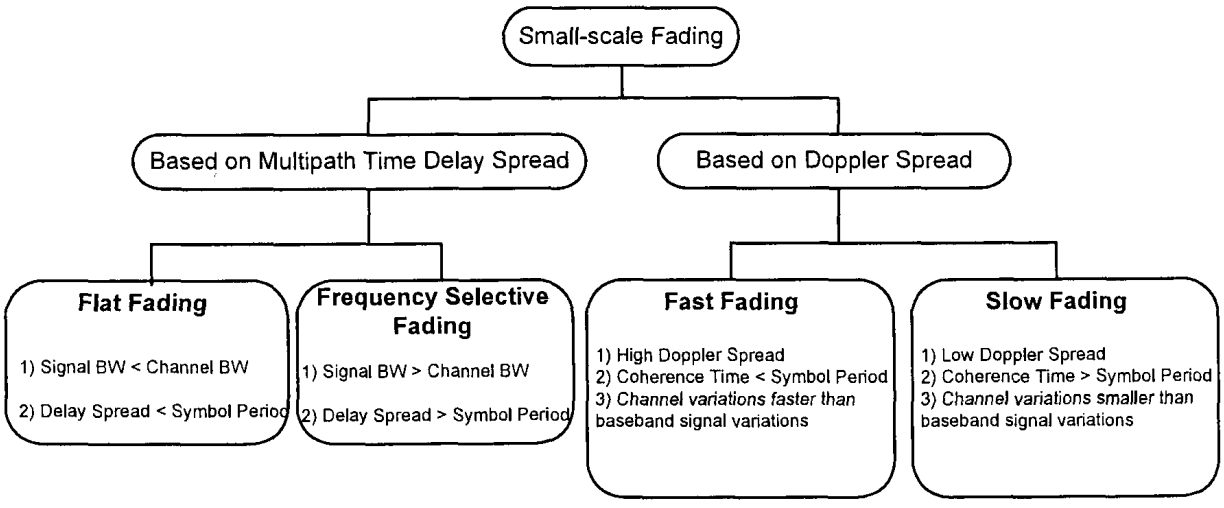

Figure 2.7: Small-scale fading types [23].

2.4.3 Rayleigh Fading Distribution

Small scale fading is called Rayleigh fading if the signal is received through many multi-paths and there is no line-of-sight component. If there are sufficiently many scatterers received at the receiver, then the channel response can be modeled as a zero-mean Gaussian process with phase evenly distributed between 0 and 2π irrespective of the distribution of the individual components according to the central limit theorem. In that case, the envelope of the received signal will have a Rayleigh distribution.

2.4.3.1 Jake's Doppler Spectrum

There are many different types of Doppler spectrum used in channel modeling. This thesis concentrates only on Jake's Doppler spectrum. Jake's Doppler spectrum was modeled by Gans [28] by analyzing the Clarke's model [29] for a mobile fading channel. Jake's Doppler spectrum model was derived from the following assumptions:

1. Radio waves propagate horizontally
2. The angle of arrival of radio waves at the receiver are uniformly distributed over $[-\pi, \pi]$
3. The receiver antenna is omni-directional

The channel auto-correlation of the Jake's model is given by,

$$R_H[m] = \frac{E[(H_{k,t} - \mu)(H_{k,t+m} - \mu)]}{\sigma^2} \tag{2.9}$$

where $E[\cdot]$ is the expected value operator, μ and σ^2 are the mean and variance of H_k, and H_k is the past channel responses of the k^{th} sub-carrier.

The channel correlation for the Jake's Model was theoretically proven to be

$$R_H[m] = J_0(2.\pi.f_D mT) \tag{2.10}$$

where $J_0(\cdot)$ is the zeroth order Bessel function of the first kind, f_D is the maximum Doppler shift and T is the OFDM symbol duration.

In this thesis, we make use of equation (2.9) instead of equation (2.10) for the following reasons:

1. In practical scenarios, it is not always guaranteed that the channel will follow the theoretical model.

2. Calculation of Doppler shift is computationally complex and can introduce delay.

2.5 Channel Equalization

Channel equalization is a technique that is used in the receiver in order to recover the distorted data due to ISI. It is implemented in either the time-domain or the frequency-domain with a symbol-by-symbol approach or sequence estimation algorithms. The transmitted signal $x[n]$ is convolved with the time-domain channel response $h[n]$ as shown in the equation (2.11)

$$y[n] = h[n] * x[n] + w[n] \tag{2.11}$$

where $*$ is the convolution operator and $w[n]$ is additive white Gaussian noise (AWGN) in time-domain.

In order to remove the effects introduced by channel, another convolution must be carried out in the time-domain. This function is called time-domain equalization.

The length of the equalizer is of the order of the time span of the channel. This type of equalizer can be expensive to implement in hardware due to the implementation of convolution. Equation (2.11) can be written in the frequency-domain as shown in equation (2.12)

$$Y(f) = H(f).X(f) + W(f) \tag{2.12}$$

where $H(f)$ is the frequency-domain channel response, $X(f)$ is the frequency-domain transmitted data and $W(f)$ is the frequency-domain AWGN.

In an OFDM system, the time domain received signal is converted to frequency-domain as a part of the process at the receiver side. Due to the periodic nature of the cyclically extended OFDM symbol, the received frequency-domain signal can be written as shown in equation (2.12). Therefore, the equalization is obtained by simple division as shown in equation (2.12) in contrast to convolution in the time-domain equalization.

$$X_R(f) = \frac{Y(f)}{H_p(f)} = \frac{X(f) + W(f)}{H_p(f)} \tag{2.13}$$

where $X_p(f)$ is the predicted channel response and $X_R(f)$ is the recovered signal at the receiver side.

The transmitted data undergoes frequency flat fading due to the splitting of the wide-band channel to multiple narrow-band channels. Frequency flat fading makes channel equalization simple compared to frequency selective fading. In addition to these advantages, the main consideration here is to predict the channel response so that it can be used to recover the data. In order to predict the channel, Pilot data which is already known to the receiver, is sent alternating with the user data to update

the receiver with new channel characteristics and to recover from errors. In this thesis, a block type (Figure. 2.8) pilot pattern is adapted for the channel prediction.

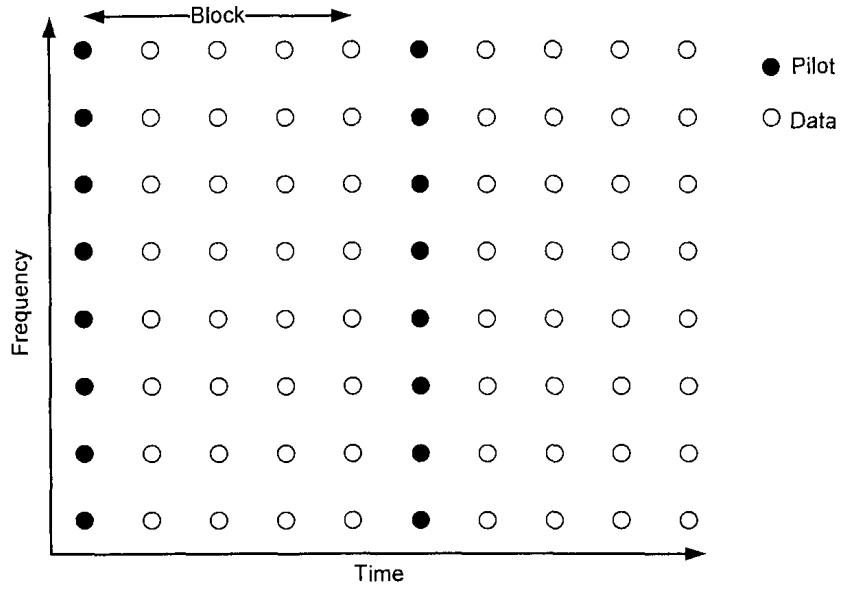

Figure 2.8: Block type pilot pattern.

2.6 Prediction of Channel Responses

As mentioned in the above section, accurate prediction of channel responses is very important for good recovery of transmitted data. In this thesis, only the frequency-domain prediction is addressed.

Of the many different frequency-domain prediction methods used, the Minimum Mean Square Error (MMSE) based prediction [30] outperforms the others in accuracy but at the expense of high computational complexity. Kalman filter based prediction of channel responses is a subset of MMSE and it provides a good trade off for the computational complexity compared to the MMSE based prediction. The following section gives a brief introduction to the Kalman filter which is applied in Chapter 3.

2.7 Introduction to Kalman Filter

A Kalman filter is a recursive predictive filter based on a state space technique and a recursive algorithm. Welch [31] provided a detailed introduction to the discrete Kalman filter. Kalman filter estimation works in the form of feedback control where first the filter estimates the process state and then obtains feedback in the form of noisy measurements and corrects itself for further estimates. Therefore, the Kalman filter estimate iterations can be grouped into two: 1) a Kalman filter Time update (or predict), where the prediction of future state is estimated from the past states, and 2) a Kalman filter measurement update (or correct), where predicted state estimates are corrected based on the received noisy measurements.

2.8 Support Vector Machine

Support Vector Machine (SVM) is a supervised classification method known as a "large margin classifier" [32]. SVM uses the training data set to find a hyperplane with the maximum margin to classify the training data samples correctly. The hyperplane with the maximum margin gives the largest separation between the two classes. The training samples that are closer to maximum hyperplane are called "support vectors". Hyperplane is estimated using support vectors only.

Once the hyperplane is estimated, a set of testing data is used to evaluate the accuracy of the decision boundary. Thereafter, the designed SVM classifies any data inputs. Fletcher in his tutorial [33] has provided a detailed explanation for finding the decision boundary using SVM.

In this thesis, SVM is used to find the modulation boundaries based on the BER of each modulation scheme.

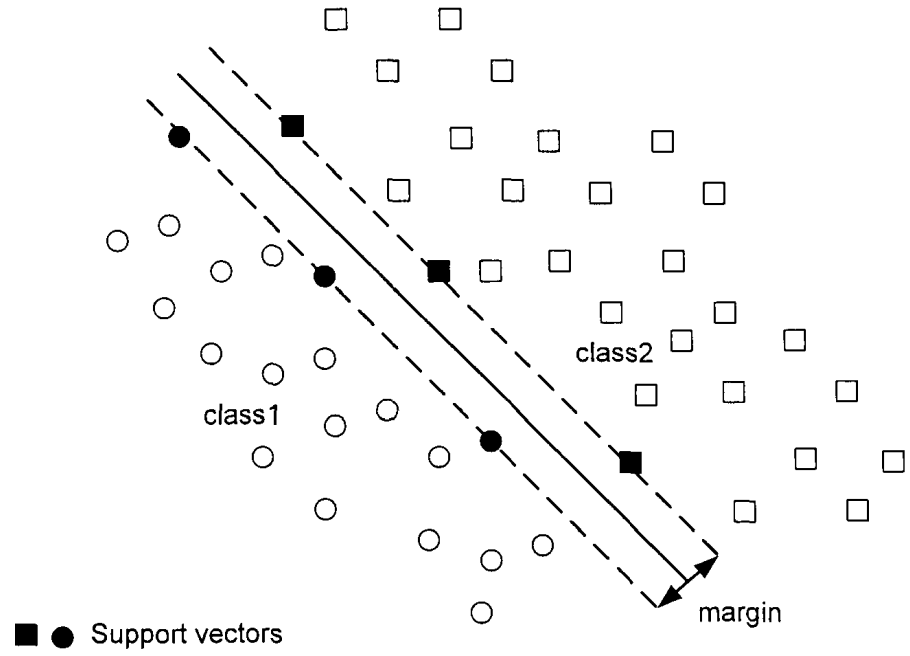

Figure 2.9: Decision boundary using linear support vector machine classifier.

2.9 Summary

In this chapter, technical background related to this thesis were introduced. First, the basics of an OFDM system and digital modulation were discussed. This was followed by an explanation of the wireless channel model and the receiver side operations. Finally, a brief introduction to Kalman filter and the the support vector machine algorithms were presented.

Chapter 3

Prediction of Channel Responses for Varying Receiver Speed

3.1 Introduction

A signal transmitted through a wireless channel undergoes severe distortion due to the following three phenomena: 1) multi-path fading, 2) Doppler shift due to the relative movement of the receiver with respect to the transmitter and 3) Gaussian noise. In order to recover the transmitted signal correctly, corrective measures need to be taken at the receiver side. Equalization is a technique used to recover the signal using channel responses. Accurate prediction of future channel responses are very important in channel equalization. This chapter focuses on recovering transmitted signal that have been distorted due to relative movement of the receiver with respect to the transmitter. Figure 3.1 shows a typical OFDM system [26] used in this chapter. Detailed explanation of an OFDM system was presented in the previous chapter.

The wireless channel considered in this chapter is a Gaussian Wide Sense Stationary-Uncorrelated Scattering (GWSS-US), frequency-selective, slow, Rayleigh fading channel with uniformly distributed angle of arrival and Jakes' model Doppler spectrum [34]. Here it is assumed that the number of resolvable multi-paths and the delay associated with each multi-path are constant for the time period considered.

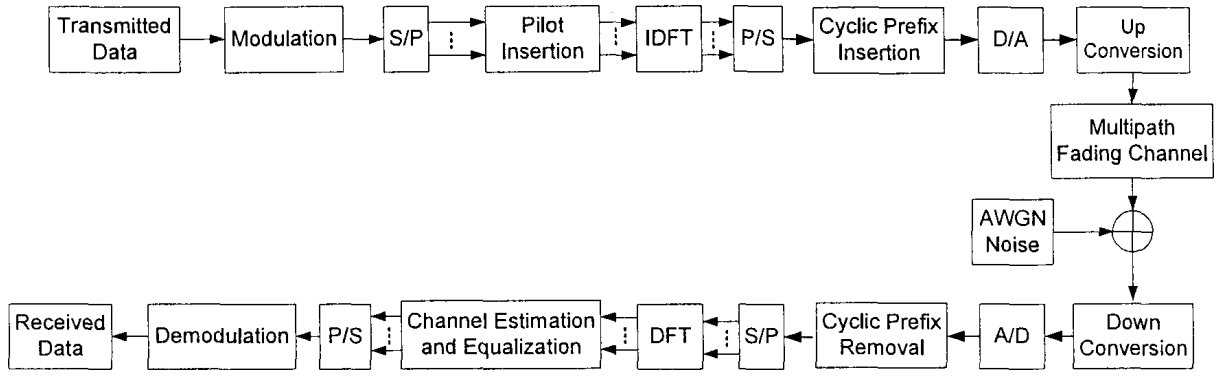

Figure 3.1: Typical OFDM system with channel predictor [26].

This chapter presents a technique that attempts to keep track of Doppler shift changes which are then used to update the Kalman filter parameters used in channel prediction. The performance of the proposed system is then compared with a system which calculates the Kalman filter parameters at fixed time intervals (Traditional method).

The proposed system provides similar BER performance compare to the traditional systems which is less than 0.001 at receiver speeds lower than 20 km/h. At receiver speeds higher than 75 km/h, the proposed system provides better BER performance compared to the traditional system. The improvement in BER performance is around 10-20% compared to system that updates the predictor parameters at fixed time intervals.

The total amount of auto-correlation calculation needed by the proposed system when the receiver move with its maximum acceleration of 9 m/s^2 is around 43 whereas, it needs 56 and 42 computations for the systems that calculates at fixed steps of every 3000th and 4000th OFDM symbol respectively. Furthermore, for the proposed system the number of computations of auto-correlation remain 43 when the acceleration or declaration is less than the maximum whereas for the other system it is increased. From these results it is evident that even though the proposed system does

not have significant improvement in BER performance, it achieves that performance with high computational efficiency.

In this chapter, a state space model of a wireless channel and a state space model application in the Kalman filter is introduced in section 3.2. A prediction of channel responses when the receiver moves with a fixed speed with respect to the transmitter is presented in section 3.3. In section 3.4, analysis and implementation of a technique that was used to keep track of the receiver speed is presented along with its potential application for predicting channel responses when the receiver moves with varying speeds. The accuracy of the predicted channel responses, performance and the computational complexity of the proposed system are investigated using simulation results in Section 3.5.

3.2 State-Space Model and Kalman Filter

Table 3.1: Kalman Filter Equation Symbols.

Symbol	Description	Matrix Size
H_n	Channel Response	
q_n	Process Noise	
Q_n	Covariance matrix of process noise	MxM
R_n	Covariance of measurement noise	Scalar
K_n	Kalman gain	Scalar
$H_{n\|n-1}$	*A-priori* estimate of channel response	Scalar
$H_{n\|n}$	*A-posteriori* estimate of channel response	Scalar
$H_{n-1\|n-1}$	Past channel responses	Mx1
$P_{n\|n-1}$	Covariance matrix of the *a-priori* error	MxM
$P_{n\|n}$	Covariance matrix of the *a-posteriori* error	MxM
X_n	Input to the channel	1xM
C_n	Kalman filter state transition matrix	MxM
Y_n	Received signal at instance n	Scalar
V_n	Measurement Noise	Scalar
A_i	1^{st} row of transition matrix coefficients	Scalar

In an OFDM system, each sub-channel can be designed using an Auto-Regressive (AR) model [10,11]. The prediction steps of channel responses for one sub-channel are discussed here and they can be extended for other sub-channels. The interpretation of the equation symbols in the this section are given in Table 3.1. The M^{th} order AR model of the sub-channel can be written as follows:

$$H_n = -\sum_{i=1}^{M} A_i H_{n-i} + Q.v_n \tag{3.1}$$

$$Y_n = X_n.H_n + w_n \tag{3.2}$$

The above state space model can be used by the Kalman filter for the prediction of channel responses. Following are the steps that are used in the Kalman filter for the prediction and estimation of channel responses.

Kalman Prediction:

$$H_{n|n-1} = C_n.H_{n-1|n-1} \tag{3.3}$$

$$P_{n|n-1} = C_n.P_{n-1|n-1}.C_nH + Q_n \tag{3.4}$$

Kalman Update:

$$G_n = X_n.P_{n|n-1}.X_n^H + R_n \tag{3.5}$$

$$K_n = P_{n|n-1}.\frac{X_n^H}{G_n} \tag{3.6}$$

$$H_{n|n} = H_{n|n-1} + K_n(Y_n - X_n.H_{n|n-1}) \tag{3.7}$$

$$P_{n|n} = P_{n|n-1} - K_n.X_n.P_{n|n-1} \tag{3.8}$$

3.2.1 Kalman Filter Parameters

3.2.1.1 Calculation of R_n

Assuming that the SNR of AWGN is already known to the receiver, the covariance of noise measurement (R_n) is calculated from equations 3.9 and 3.10.

$$\sigma_N^2 = \frac{1}{10^{\frac{SNR}{10}}} \tag{3.9}$$

$$R_n = \frac{{\sigma_N}^2}{2} \tag{3.10}$$

where ${\sigma_N}^2$ is the noise variance.

3.2.1.2 Calculation of C_n and Q_n

Most channel response prediction methods proposed in the literature assume that the Doppler shift of a fading channel is known (or pre-calculated) at the receiver end and they use the theoretical formula in equation 2.10 to estimate the auto-correlation of channel responses. This estimated auto-correlation is then used to find the Kalman filter parameters C_n and Q_n. In practical systems, it is not always guaranteed that the auto-correlation of the channel responses follows the theoretical formula which is a drawback.

In the proposed system, A_i's in C_n matrix and Q_n are calculated by applying the Yule-Walker method [9] to the auto-correlation of channel responses estimated by applying equation 2.9 on the estimated past channel responses. The state transition matrix C_n in the Kalman filter prediction steps can be written as in equation 3.11. The sizes of matrices C_n and Q_n are determined by the order of the Kalman filter (M).

$$C_n = \begin{bmatrix} -A_1 & -A_2 & \cdots & -A_{M-1} & -A_M \\ 1 & 0 & \cdots & 0 & 0 \\ 0 & 1 & \cdots & 0 & 0 \\ \vdots & \vdots & \ddots & \vdots & \vdots \\ 0 & 0 & \cdots & 1 & 0 \end{bmatrix} \tag{3.11}$$

3.3 Prediction of Channel Responses for the Receiver Moving with a Fixed Speed

Step1: Initialize the Kalman filter with $H_{n|n-1} = 0$ and $P_{n|n-1} = I$, where I is the identity matrix of same size as the AR order.

Step2: Calculate the Kalman filter parameters, C_n, Q_n, and R_n

Step3: At the reception of an OFDM symbol, the following Kalman update and prediction steps are made:

1. Kalman Update
   (a) If the received symbol is a pilot symbol
   - $H_{n|n} = Y_n / X_{n,P}$
   - $P_{n|n} = P_{n|n-1} - K_n . X_{n,P} . P_{n|n-1}$

   (b) If the received symbol is a data symbol
   - $X_n = Y_n / H_{n|n-1}$
   - $G_n = X_n . P_{n|n-1} . {X_n}^H + R_n$
   - $K_n = P_{n|n-1} . {X_n}^H / G_n$
   - $H_{n|n} = H_{n|n-1} + K_n (Y_n - X_n . H_{n|n-1})$
   - $P_{n|n} = P_{n|n-1} - K_n . X_n . P_{n|n-1}$
2. Kalman Prediction
   - $H_{n|n-1} = C_n . H_{n-1|n-1}$*
   - $P_{n|n-1} = C_n . P_{n-1|n-1} . {C_n}^H + Q_n$

   *For the multi-step prediction, the predicted $(n+1)^{th}$ channel response is used with estimated channel responses to predict $(n+2)^{th}$ channel response.

Step4: Refinement of predicted channel responses using channel auto-correlation along the frequency axis.

Step4: Go back to step 2.

Algorithm-1: Prediction of channel responses for fixed receiver speed [11]

In this section, the prediction of channel responses for a receiver moving with a constant speed is considered. Therefore, the Kalman filter parameters are considered to be constant. Algorithm-1 shows the steps of the prediction algorithm used for the receiver moving with a fixed speed. Here, it is assumed that SNR of the channel is

known to the receiver.

3.4 Prediction of Channel Responses for a Receiver Moving with Varying Speeds

As discussed in Chapter 2, the maximum Doppler shift observed by the receiver is proportional to the speed of the receiver with respect to the transmitter. The auto-correlation of channel responses depends on the maximum Doppler shift experienced by the receiver. Therefore, the Kalman filter parameters C_n and Q_n which are estimated using the auto-correlation of channel responses are also depend on the relative speed of the receiver. For the receiver moving with varying speed, the Kalman filter parameters are need to be updated based on the speed changes of the receiver (or correspondingly significant change in auto-correlation of the channel responses). Therefore, in order to adapt the Kalman filter parameters for varying receiver speeds, it is necessary to identify the significant changes in the auto-correlation of channel responses and update the Kalman filter parameters accordingly.

3.4.1 Analysis of Receiver Speed and Nulls in Received Signal Envelope

A moving receiver receives a large number of reflected and scattered waves. These waves accumulate together to create the instantaneous received signal. For a single carrier system, the signal envelope (or power) seen by a moving receiver is a random variable which depends on the location of the receiver because of wave addition and cancelation effects. Figure 3.2 [23] shows an example of a single carrier received signal envelope of a flat rayleigh fading signal while the receiver is in motion. Here,

although the fading is a random process, deep fadings (or nulls) have a tendency to occur approximately every half wavelength distance [23,35].

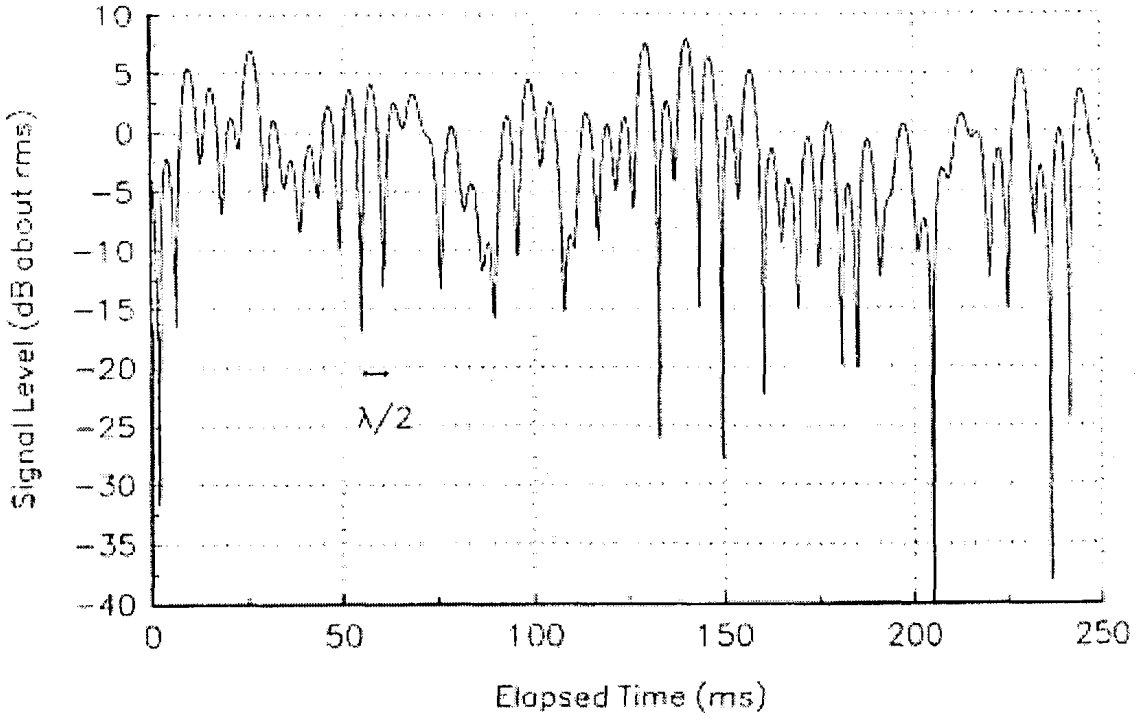

Figure 3.2: A typical Rayleigh fading envelope at 900 MHz [23].

As stated in the previous chapter, coherence time (T_c) is inversely proportional to maximum Doppler shift (f_D) (see equation 2.8). If the speed of the receiver is v m/s, rewriting equation 2.8

$$T_c = \frac{0.423}{f_D} = \frac{0.423\,c}{v\,F_c} \tag{3.12}$$

where $f_D = v\,F_c/c$, F_c is the carrier frequency and c speed of the light.

Average distance traveled by a receiver between two nulls (or two deep fadings) of the received signal envelope is approximately $\lambda/2$ and the coherence time (T_c) is given by the time taken to travel $\lambda/2$ distance [23,35]. The number of nulls in the received signal envelope of a receiver traveling at a constant speed is given by

$$N_n \approx T_{tot}/T_c \tag{3.13}$$

where T_{tot} is the total time considered for the null count. From equations 3.12 and 3.13, following can be derived:

$$N_n \approx \frac{T_{tot}\, f_D}{0.423} \tag{3.14}$$

$$N_n \propto f_D$$

3.4.1.1 Null Analysis for Multi-carrier System

In multi-carrier system like OFDM, each sub-channel can be considered a narrow band flat fading channel since the bandwidth of the each subcarrier is smaller than the coherence bandwidth of the channel [23]. Time-varying wireless channel can be written as [36]

$$h_c(t,\eta) = \sum_{p=0}^{L-1} \gamma_p(t)\delta(\eta - \eta_p(t)) \tag{3.15}$$

where $\eta_p(t)$ is the delay, $\gamma_p(t)$ is the complex amplitude of the p^{th} multi-path tap, and L is the number of propagation paths. Assuming a far-field discrete scatterer model, $\gamma_p(t)$ can be further decomposed as

$$\gamma_p(t) = \sum_{r=0}^{M_p-1} a_{r,p} e^{j2\pi\nu_{r,p}(t)t} \tag{3.16}$$

where M_p is the number of rays contributing to the p^{th} path, and $a_{r,p}$ and $\nu_{r,p}(t)$ are the complex amplitude and Doppler frequency, respectively, for the r^{th} ray in

the p^{th} path. Here, the random phase from the complex exponentials have been incorporated into $a_{r,p}$ and the time delays and Doppler frequencies are all dependent on time. However, we can assume that the time delay $\eta_p(t)$ and Doppler frequency $\nu_{r,p}(t)$ parameters vary slowly when compared to the OFDM symbol time, and can be considered constant within the estimation and prediction time horizons. Combining (3.15) and (3.16) and taking its Fourier transform,

$$H_c(t,f) = \sum_{p=0}^{L-1} \sum_{r=0}^{M_p-1} a_{r,p} e^{j2\pi\nu_{r,p}t} e^{-j2\pi\eta_p f} \tag{3.17}$$

where $H_c(t,f)$ is the frequency response of the time-varying channel.

Assuming that the OFDM system with symbol period T_{sym} and subcarrier spacing Δf have proper cyclic extension and sample timing, the sampled channel frequency response at the k^{th} subcarrier of the n^{th} OFDM block can be expressed as

$$\begin{aligned} H(n,k) &= H_c(nT_{sym}, k\Delta f) \\ &= \sum_{p=0}^{L-1} \sum_{r=0}^{M_p-1} a_{r,p} e^{j2\pi(f_{r,p}n - \tau_p k)} \end{aligned} \tag{3.18}$$

where $f_{r,p} = \nu_{r,p} T_{sym}$ is the normalized Doppler frequency and $\tau_p = \eta_p \Delta_p f$.

This multi-path fading effect on k^{th} subcarrier is similar to that of a single carrier signal. Therefore, each received sub-carrier signal undergoes a similar type of fading to that of a single carrier signal which undergoes flat fading. Re-writing the equation 3.12 by replacing single carrier frequency by subcarrier frequency

$$T_c = \frac{0.423\,c}{v\,F_{c,k}} = \frac{0.423}{f_{D,k}} \tag{3.19}$$

where $F_{c,k}$ is the k^{th} subcarrier frequency and $f_{D,k}$ is the maximum Doppler shift observed at the k^{th} subcarrier.

Using the equations (3.13) and (3.19)

$$N_n \approx \frac{T_{tot}\, f_{D,k}}{0.423} \tag{3.20}$$

$$N_n \propto f_{D,k}$$

This property is validated using the simulation results. A simulation is carried out for a duration of 20,000 OFDM symbol period. First, the received OFDM signal is converted to frequency domain discrete signal by applying FFT. Then one subcarrier signal is converted back to the time domain signal and finally performing the null count on the time-domain signal of a subcarrier for a fixed time interval equal to 3000 OFDM symbols (0.24 s). Figure 3.3 shows the mean (μ_N) and variance (σ_N) of the null counts for different maximum Doppler shifts observed at that subcarrier (receiver speeds). Here, it can be seen that the average null count (μ_N) is proportional to the maximum Doppler shift and the variance is less than 2 for the maximum Doppler shift considered.

3.4.2 Detection of Nulls in OFDM Subcarrier Signal

There are many algorithms used to find the null points (possible local minima). The simplest and fastest algorithm for this real time null detection is the first derivative test. First, the derivative of one subcarrier signal envelope (f') is calculated. Then, the points where the sign of f' changes from negative to positive is identified as a

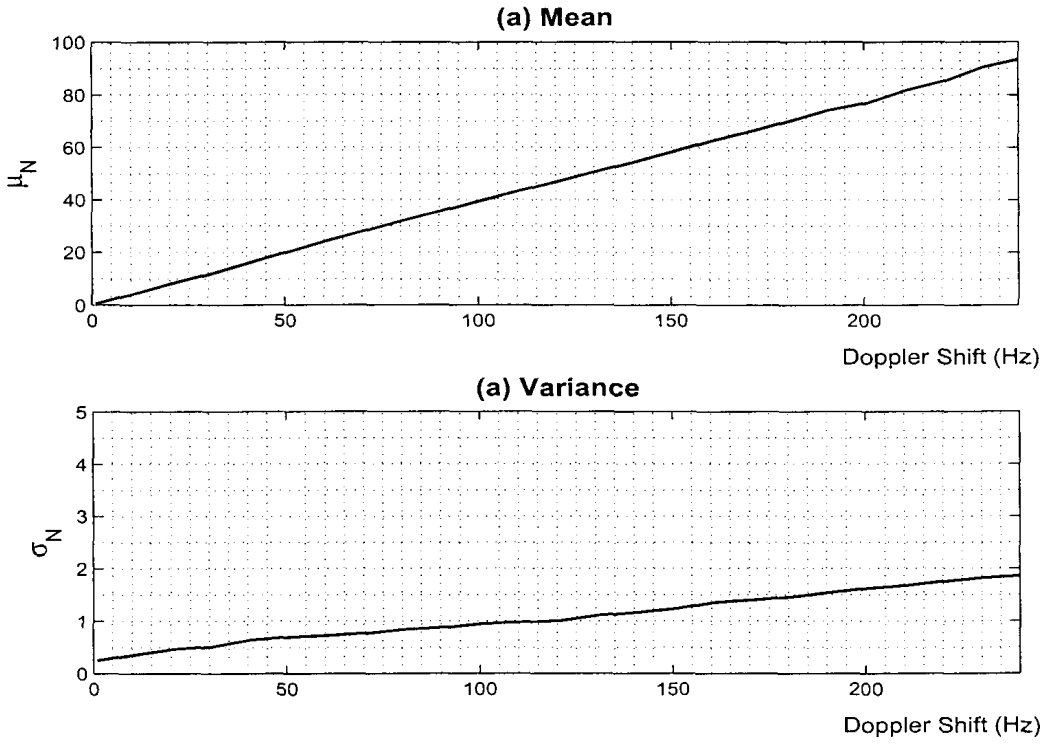

Figure 3.3: (a) Mean and (b) variance of null counts vs. Doppler shift for a fixed time duration.

null point. It is not always possible to detect the nulls using the first derivative test method only, especially when there is noise added to the received signal.

The signal received at the receiver side is affected by white Gaussian noise. It is necessary to filter out this noise before using the envelope of the subcarrier signal to estimate the number of nulls. Figure 3.4 shows a snapshot of received noisy signal at an OFDM subcarrier and the filtered signal. The fundamental frequency component of the subcarrier signal envelope is equal to the maximum Doppler shift observed at that subcarrier. Therefore, a digital Infinite Impulse Response (IIR) low pass filter with a cut-off frequency around the maximum Doppler shift is used to filter the noise. Thereafter, the number of nulls in the subcarrier signal envelope is calculated.

The possible shapes of nulls observed in the filtered subcarrier signals are shown in Figure 3.5. Following criteria are used to detect those possible nulls:

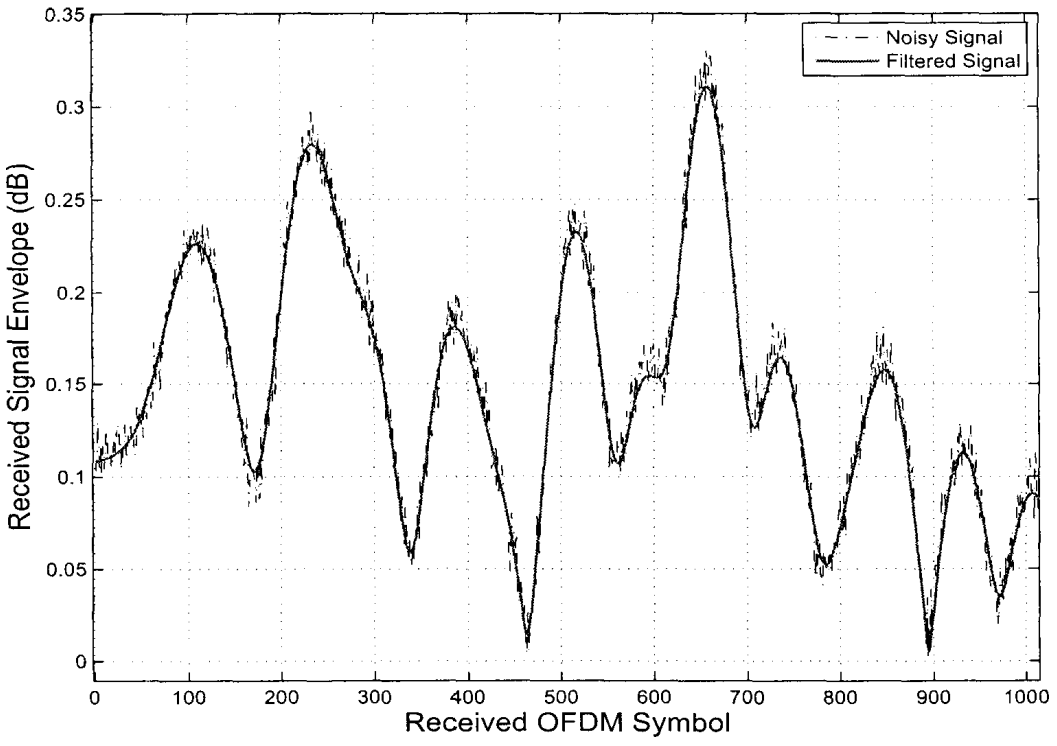

Figure 3.4: Snapshot of one subcarrier noisy signal and filtered signal.

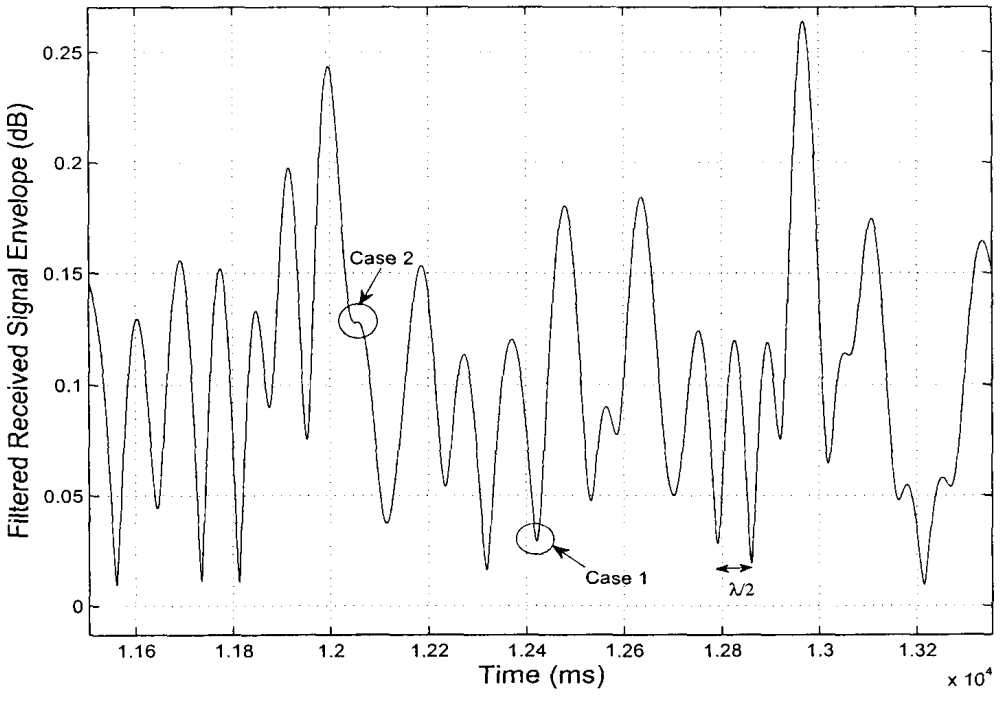

Figure 3.5: Received multi-path OFDM signal in one subcarrier.

Case1: Local minimum point (Figure 3.6)

- Sign of first derivative changing from negative to positive.

Case2: Stationary points of inflection (Figure 3.6)

- The stationary points of inflection are found using either of the following conditions: 1) f' is zero and the sign of the second derivative (f'') changes from negative to positive (Figure: 3.6 Case: 2a or 2) f' is zero and the sign of f'' changes from positive to negative (Figure 3.6 Case: 2b).

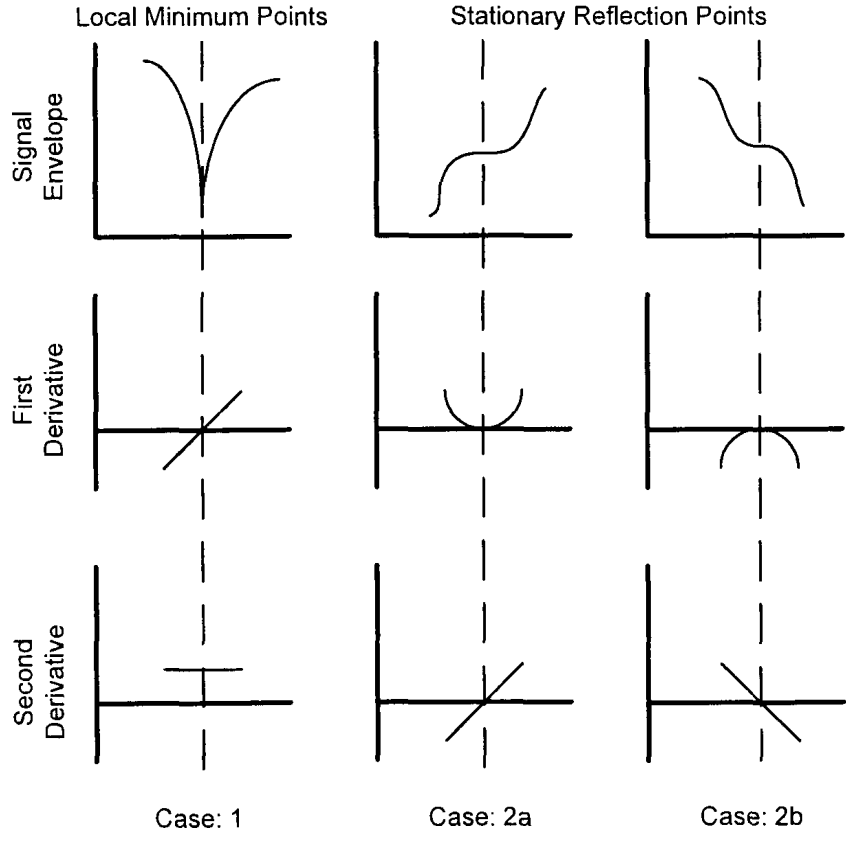

Figure 3.6: Identifying the points of reflections

3.4.3 Identification of Channel Correlation Changes

Changes in auto-correlation of channel responses are heavily dependent on Doppler shift. The variations in auto-correlations of the channel responses are smaller for lower values of Doppler shifts. For moderate Doppler shifts, the auto-correlations of channel responses vary moderately with the change in Doppler shifts and for higher Doppler shifts, they vary drastically even for small change in Doppler shift. Figure 3.7 shows the auto-correlation variation for different Doppler shifts. The auto-correlation is drawn for speed difference of 10 km/h. From the Figure 3.7 the auto-correlations of channel responses can be defined as highly correlated, moderately correlated or less correlated for lower, moderate and higher Doppler shifts respectively. Therefore, the main consideration for the proposed system is to identify the point at which the auto-correlation of the channel responses changes significantly based on current Doppler shift and to update the Kalman filter parameters based on new auto-correlation of the channel responses. These updated Kalman filter parameters are then used for future channel predictions.

Based on Figure 3.7, the total speed range under consideration is divided into three categories: low speed (0-40 km/h), moderate speed (40-75 km/h) and high speed (>75 km/h). The speed ranges are taken considering the vehicle speeds in different conditions like city area where the speed is around 40km/h or less, urban area where the speed can vary up to 75km/h and highway where the speed is more than 75 km/h. Different adaptive thresholds for the null counts (N_{Th}) are used for identification of channel correlation changes [Table. 3.2].

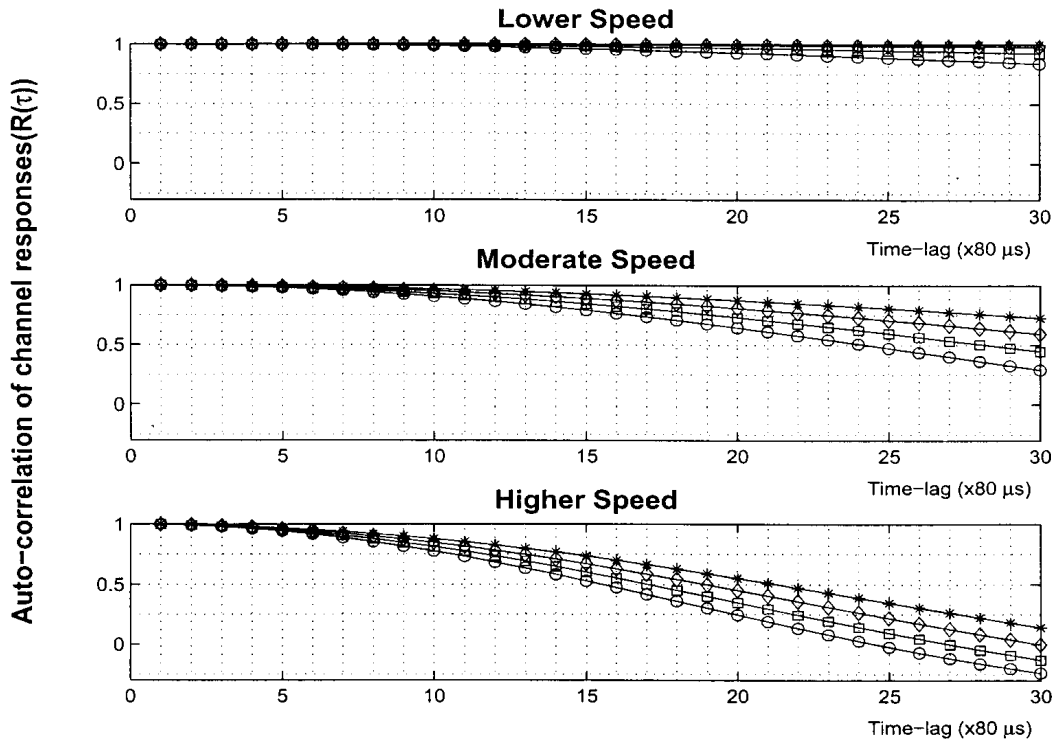

Figure 3.7: Comparison of correlation of channel responses for different receiver speeds.

Table 3.2: Speed range and channel correlation identification.

Speed Range (km/h)	Doppler Shift (Hz)	Null Variation Threshold (N_{Th})
0 – 40	0 – 70.4	$N_{Th,sp1}$
40 – 75	70.4 – 132	$N_{Th,sp2}$
>75	>132	$N_{Th,sp3}$

3.4.4 Proposed Adaptive Prediction Algorithm

Using the background information presented in previous sections, an adaptive prediction system for a receiver moving with varying speeds is developed in this section. Figure 3.8 shows the block diagram of the introduced channel predictor subsystem in a traditional OFDM system shown in Figure 3.1.

The channel predictor subsystem shown in Figure 3.8 has two main blocks namely, nulls detection and channel prediction. When an OFDM signal is received

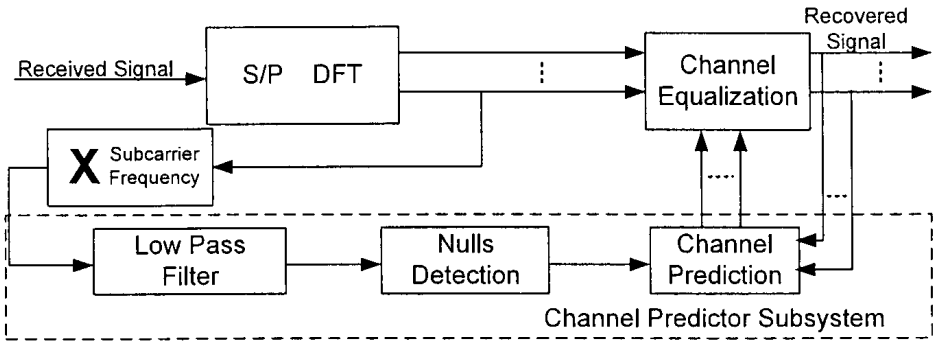

Figure 3.8: Proposed predictor subsystem.

at the receiver side, first it is converted to frequency domain signal as it is done in a conventional OFDM receiver. Then the converted signal of one subcarrier is extracted and again converted back to time-domain signal. This is done by multiplying each symbol in one subcarrier with $e^{(j2\pi f_{c,k})}$, where $f_{c,k}$ is the subcarrier frequency. Time-domain subcarrier signal is then filtered to remove the AWGN present in the signal and fed to nulls detection block for the detections of nulls (as discussed in section 3.4.2). The nulls detection block identifies the nulls in the time-domain subcarrier signal envelope and counts the total number of nulls at a fixed time interval. The updated null count (N_n) is then fed to channel prediction block at the reception of each OFDM symbol for further processing.

In the channel prediction block, Initially the frequency-domain auto-correlation of channel responses (R_H) is calculated from the past estimated channel responses. Following the calculation of the auto-correlation, the channel prediction block updates the threshold for the null count (N_{Th}) using Table 3.2 based on the receiver speed. Here, the speed range of the receiver is estimated using the estimated auto-correlation of channel responses. The nulls count at the time of calculation of auto-correlation of channel responses (N_c) is also updated using N_n. Then the Yule-Walker method is applied on calculated auto-correlation of channel responses to estimate the Kalman

filter parameters (C_n, Q_n, and R_n).

At the reception of each OFDM symbol, the nulls detection block detects the nulls in the filtered time-domain subcarrier signal envelope and updates nulls count (N_n). The updated N_n is fed to channel prediction block where it is compared with N_c and N_{Th} according to the equation (3.21).

$$|N_c - N_n| > N_{Th} \tag{3.21}$$

If equation 3.21 is satisfied, then the channel auto-correlation and Kalman filter parameters are re-calculated and updated. N_{Th} is then updated based on the receiver speed and N_c is updated using N_n. If equation 3.21 is not satisfied, then the channel prediction block uses the old Kalman filter parameters to predict the future channel responses and till the condition given in equation 3.21 is satisfied. This process is repeated throughout the transmission period from the transmitter to the receiver. Figure. 3.9 shows the flow chart of the proposed prediction algorithm.

3.5 Simulation Results and Analysis

To evaluate the performance of the proposed system, numerical simulations have been carried out using Matlab. Table 3.3 summarizes the OFDM system and channel parameters used in this system. It is assumed that the transmitter and the receiver are fully synchronized with each other. The channel used here is a frequency selective slow Rayleigh fading channel. It can be assumed that the sub-channels undergo flat fading which makes the channel predictor sub-system simple compared to the system for frequency-selective fading channels. The prediction Mean Square Error (MSE) and the Bit Error Rate (BER) are obtained by varying SNR of the channel and

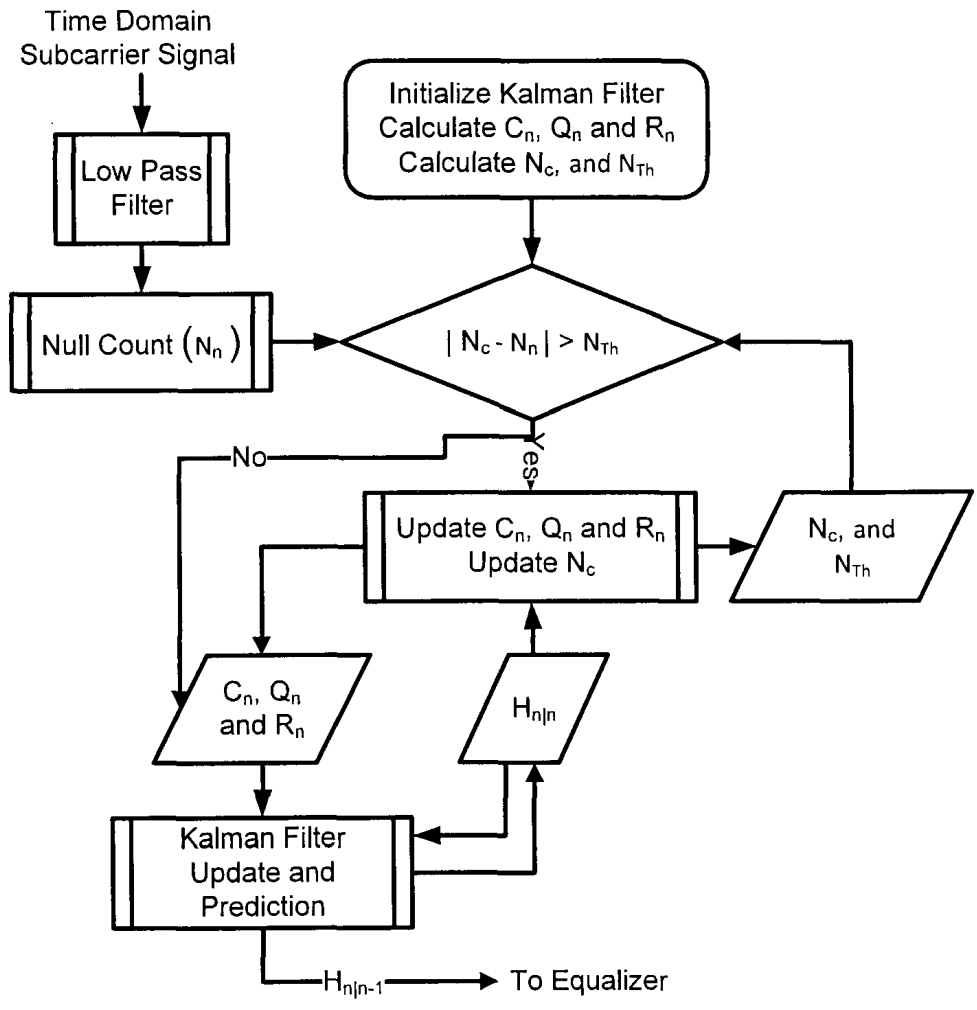

Figure 3.9: Flow chart for channel prediction for varying receiver speed.

the relative speed of the receiver with respect to the transmitter. Initially 100 pilot OFDM frames are transmitted to train the receiver for a given channel condition. Thereafter, typical OFDM frames are transmitted and the system performance is evaluated. An OFDM frame consists of 10 OFDM symbols in which the first OFDM symbol is a pilot symbol.

Table 3.3: OFDM and Channel Parameters

Sampling Frequency	1MHz
Channel Model	Frequency-selective Rayleigh fading [12]
Modulation	M-PSK
Number of subcarriers	64
Cyclic prefix length	16
Pilot Arrangement	Block type (one per frame)
OFDM symbols per frame	10
Kalman filter order	3

3.5.1 Simulation Results for Fixed Receiver Speed Scenarios

For fixed receiver speed simulations, performance is evaluated by sending 70,000 OFDM symbols of which 10% are pilot symbols. All the sub-carriers are used for data transmission and it is assumed that all the 64 sub-carriers are assigned to one user.

Figure. 3.10 shows a snap shot of an actual channel response and the predicted channel response in the presence of noise by the proposed system. Figures. 3.11 and 3.12 show the MSE versus energy-per-bit to noise power ratio (E_b/N_o) for Q-PSK and 16-PSK modulation respectively and Figures 3.13 and 3.14 show the MSE versus receiver speed (in km/h) for QPSK and 16-PSK modulation respectively. These graphs shows that the MSE and BER increases with the increase receiver speed and/or decrease in E_b/N_o.

Figures 3.15 and 3.16 show the BER versus E_b/N_o for QPSK and 16-PSK modulation respectively and Figures 3.17 and 3.18 show the BER versus receiver speed for the QPSK and 16-PSK modulation respectively. From these plots it is evident that BER also has a similar pattern compared to the MSE for different E_b/N_o and receiver speeds.

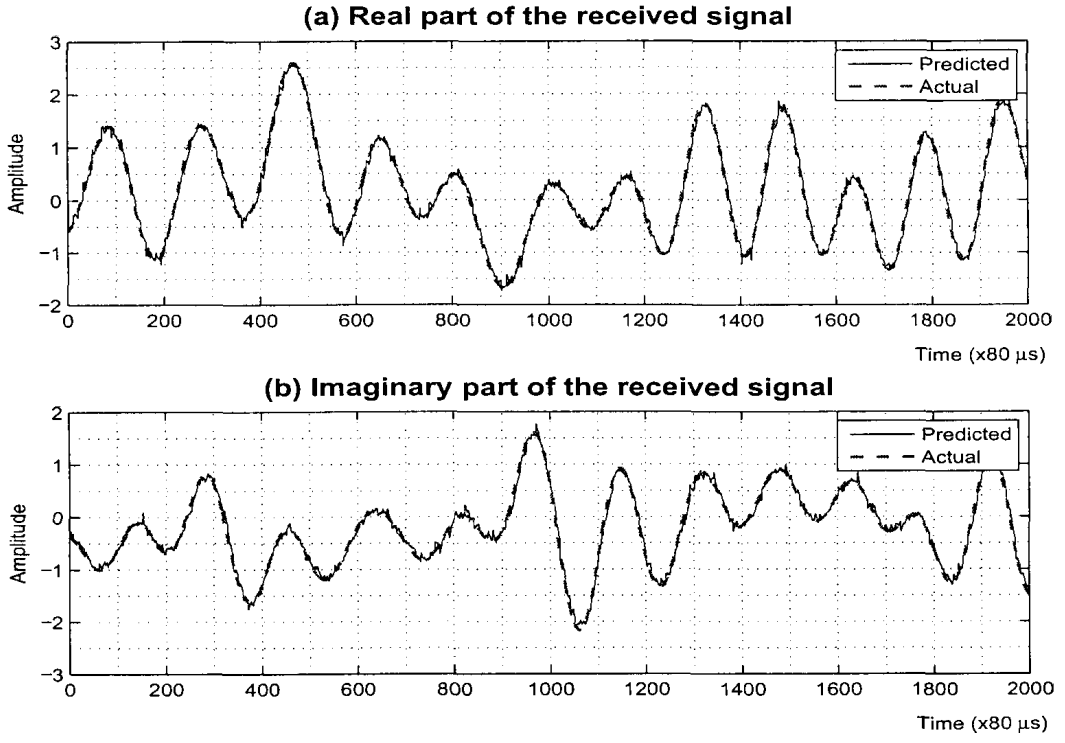

Figure 3.10: Snap shot of actual and predicted channel responses.

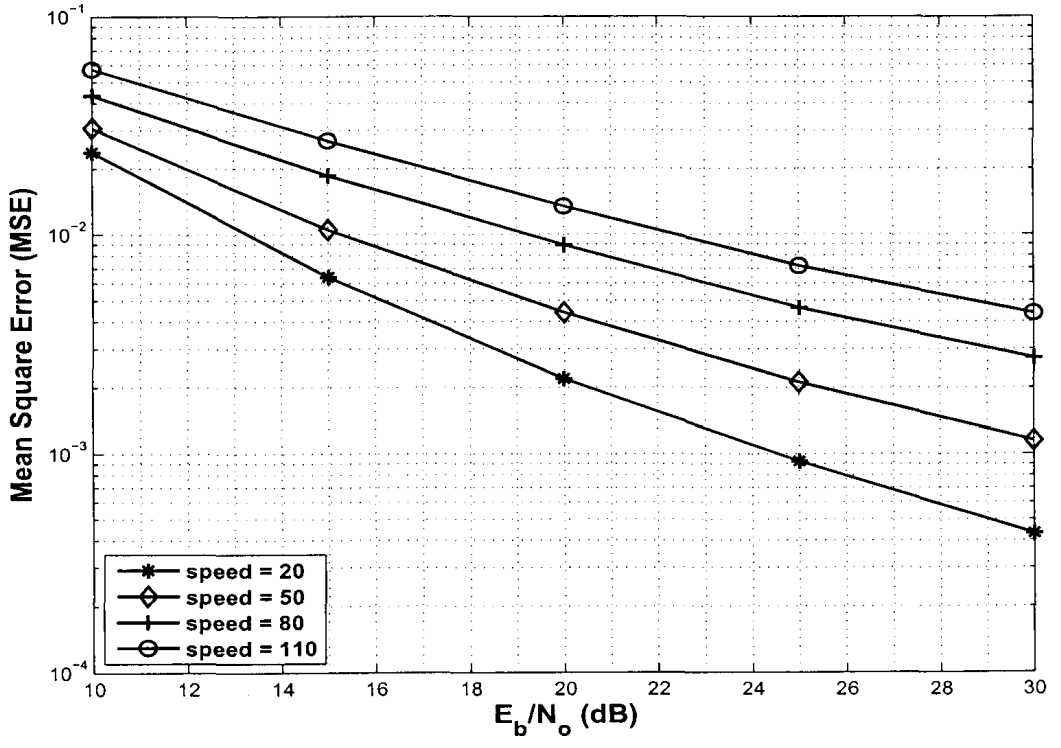

Figure 3.11: Mean square error vs. E_b/N_o for QPSK modulation.

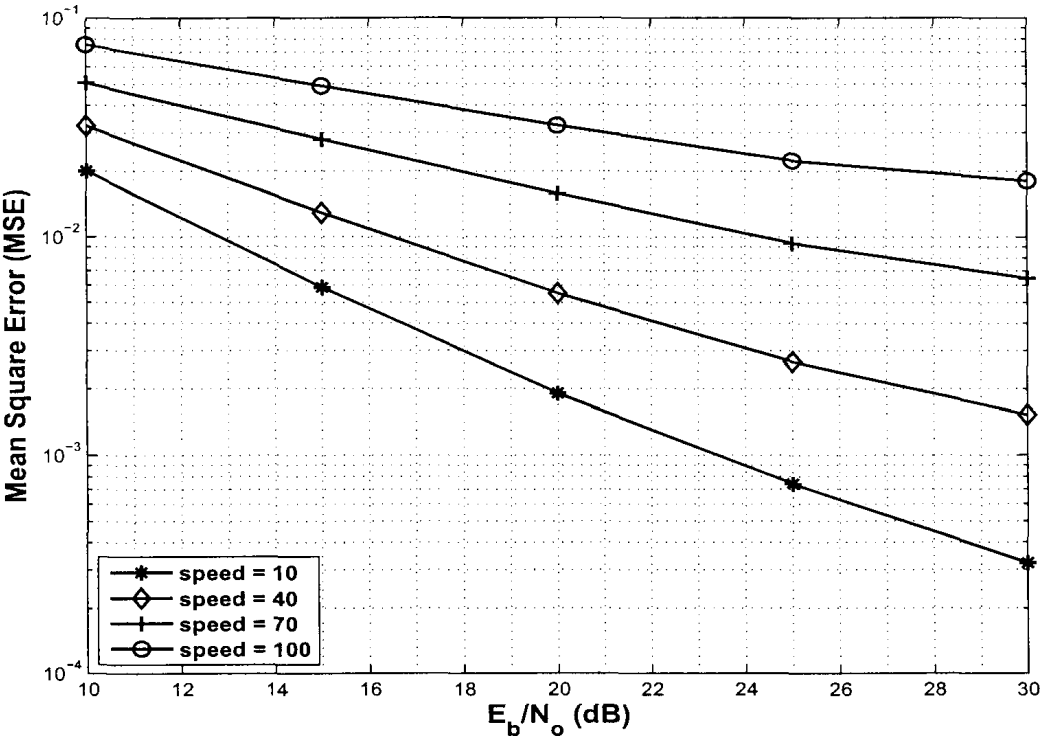

Figure 3.12: Mean square error vs. E_b/N_o for 16-PSK modulation.

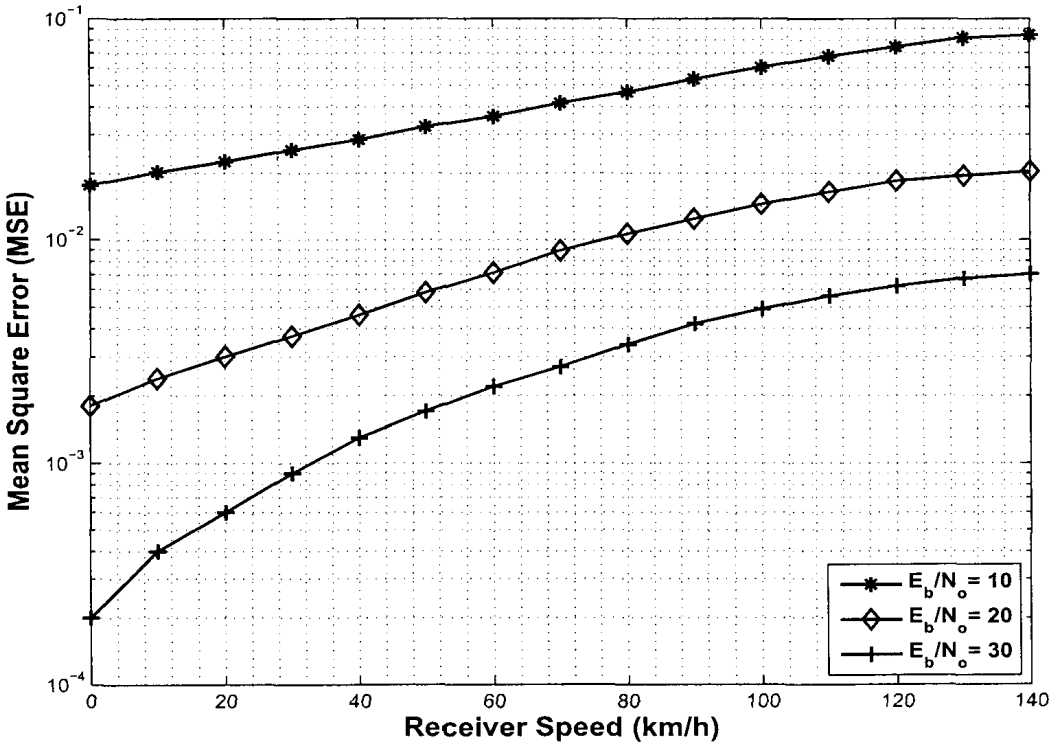

Figure 3.13: Mean square error vs. receiver speed for QPSK modulation.